




Efficient 2D Processing of 1D Sensor Signals

Ömer Nezir Gerek^(✉) 

Department of Electrical and Electronics Engineering, Eskisehir Technical University,
26555 Eskisehir, Turkey
ongerek@eskisehir.edu.tr

Abstract. Signal processing had been the flagship technology behind the intelligent systems for applications ranging from multimedia to biomedicine, from renewable energy systems to telecommunications. It is customary to apply processing tools dedicated for the natural sensor output. For instance, audio signals are processed with 1D techniques, whereas captured images are processed via 2D methods. On the other hand, many 1D sensor outputs exhibit an intrinsically cyclic behavior. Solar radiation recordings, captured line voltage values, cardiac potential, electric consumption, etc. are all fine examples to 1D signals which already have the quasi-periodicity. Recent research efforts of the authors have shown that the cyclic behavior of such signals may help a 2D rendition of the same information, provided that the natural period is accurately determined and assigned as the “width” of the 2D matrix. Experimental results indicate improved efficiency of 2D representation in terms of modelling, prediction and error detection. This work aims to provide a mathematical reasoning to the efficiency of such 2D rendition over 1D processing in terms of reduced autocorrelation orders.

Keywords: 2D rendition · Signal modeling · Efficient sensor data processing

1 Signals with Cyclic Behavior

Regular 1D sensors generate continuous time (CT) or discrete time (DT) signals at their output stages for further processing. For simplicity, and for the sake of computer processing capability, let us consider that the sensors generate a DT signal with a sampling period of T_s seconds, for a total duration of T_{Max} seconds, making an eventual array (denoted by the vector, \mathbf{x}) of length $N = T_{Max}/T_s$. In a majority of cases, the vector does not exhibit any form of periodicity (or a quasi-periodicity). Speech waveforms and wind speed data are examples to such. However, for *some* cases, the data tends to have a weak or strong repetitive nature. In the following subsections, we will exemplify some of the useable and almost periodic signals that can be acquired in the form of 1D signals.

1.1 Solar Radiation Signals

Thanks to the precise rotation of planet earth, the solar extra-terrestrial irradiance on a given geo-location of earth surface can be accurately calculated [1, 2]. Assuming the

solar time t_s as a minute count, the hour-angle can be defined as:

$$\omega = \frac{2\pi}{24} \left(\frac{t_s}{60} - 12 \right). \tag{1}$$

Let the sensor tilt (from horizontal tangent) be β (can be zero), azimuth angle is γ and the latitude is ϕ . Due to the geo-tilt, the declination angle must be separately calculated as:

$$\delta = 0.41 \times \sin \left(2\pi \frac{284 + d}{365} \right) \tag{2}$$

Abstract. For the Northern Hemisphere. Combining the terms, the angle of incidence (a.k.a. zenith angle) satisfies:

$$\cos\theta_z = \cos\phi\cos\delta\cos\omega + \sin\phi\sin\delta, \tag{3}$$

which yields a global extra-terrestrial solar radiation expression of:

$$G_0 = G_{sc} \left(1 + 0.033\cos \left(\frac{2\pi d}{365} \right) \right) \cos\theta_z \tag{4}$$

for the day, d , with $G_{sc} = 1367 \text{ W/m}^2$.

Despite the relative complexity of the expression, it is clear that the radiation term is eventually periodic with a period of 1 year. However, things get more interesting if the quasi-period of 1 day is considered. Because then, rendition of an hourly (or minute-wise) solar radiation becomes almost the same for adjacent dates (Fig. 1 and Fig. 2).

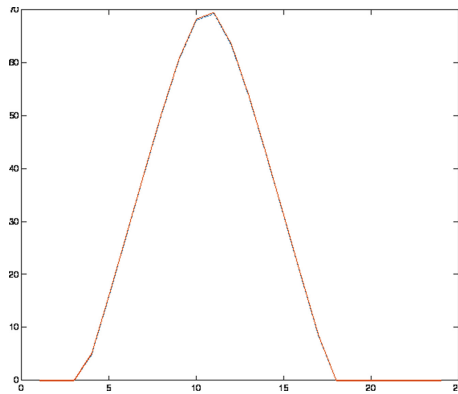


Fig. 1. Extraterrestrial solar radiation in 2005 over location in UK for 26th (solid red) and 27th (blue dash-dot) of July [3]. The curves are almost indistinguishable. (Color figure online)

Since the daily variations are expected to be minimal, the 2D rendition of the solar radiation data is expected to make perfect sense when a period of 24 h is selected as the width of the 2D matrix, where every day makes a row of the 2D matrix. Since the

extraterrestrial radiation is a deterministic signal with no random component (due to facts such as cloudiness, rain, dust, environmental reflections, etc., the 2D rendition should, in fact, be applied to the measurement sensor outputs. Consider an hourly observation of fixed panel solar radiation in Eskisehir region is rendered for a complete year of 2005 in Fig. 3 [4, 5].

The congested plot in Fig. 1 merely shows any meaningful information regarding the hourly changes. Nor is it of any help in constructing an hourly prediction model. Now, with the above-mentioned idea, if the data is rendered in 2D (with a width corresponding to 24 h), the new representation becomes as in Fig. 4.

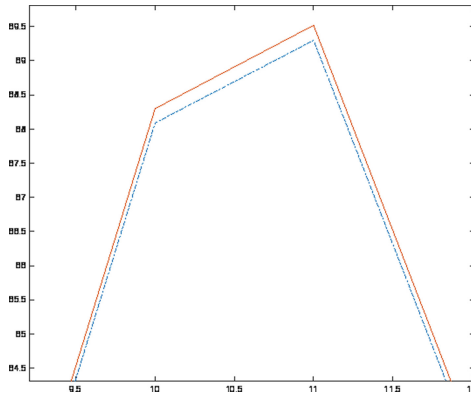


Fig. 2. A zoom-in of Fig. 1 shows the very slight difference in values.

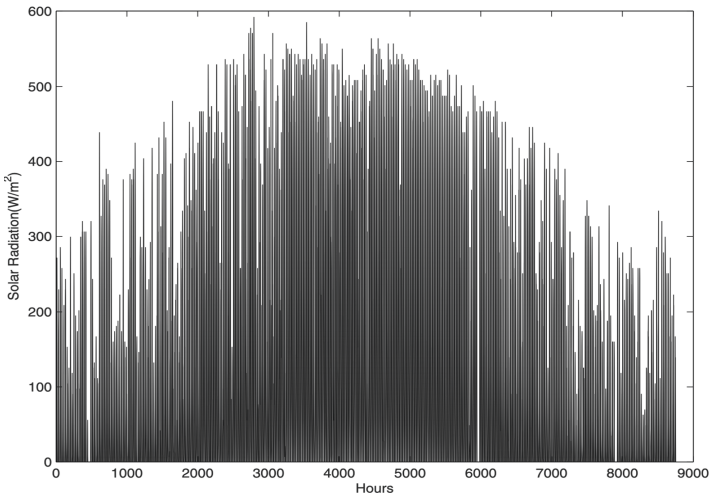


Fig. 3. 1D plot of hourly solar radiation data collected in Eskisehir in 2005.

The new 2D representation of the *same* data instantly provides a new insight and possibilities for modelling and analysis tools. Even the stochastic components of the 2D data due to atmospheric and meteorological phenomena seem to pertain for multiple days, providing a relation to the *vertical* (daily) axis. Therefore, the new axis provides an extra degree of freedom for analysis or representation purposes. The linear and neural models in [4] and spectral models in [6, 7] have already proven to be successful, yet this application constitutes only one example for the possibility of the 2D rendition.

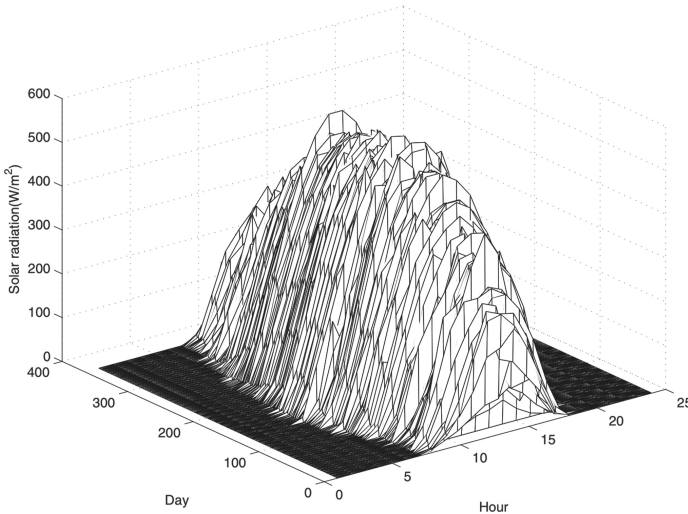


Fig. 4. 2D rendition of the hourly solar radiation data in Fig. 3.

1.2 Line Voltage and Power Quality Signals

An intrinsically periodic signal is the well-known line voltage waveform, which happens to have a frequency of 50 or 60 Hz (correspondingly 110 V or 220 V RMS) according to the regulations of the available country. Therefore, high resolution digitized voltage waveforms constitute a perfect candidate for 2D rendition as illustrated in Fig. 5. Following a power quality experiment in our laboratories and recording the voltage values at 20 kHz sampling rate, the 2D rendered data are shown in mesh plot and in the gray-scale image form in Fig. 6(a) and (b), respectively. It must be noted that the 2D rendition carries valuable information, not only revealing the power quality events, such as sag and arcing faults, but also clearly showing the very slightly lower frequency of the voltage (only a tad slower than 50 Hz, which is almost impossible to accurately detect using 1D methods) [8]. It was also found efficient to use this representation for the compression, transmission and storage of the recording [9, 10].

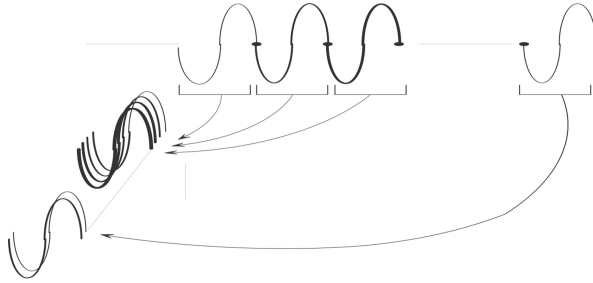


Fig. 5. 2D rendition of the periodic voltage waveform by stacking each period to a row.

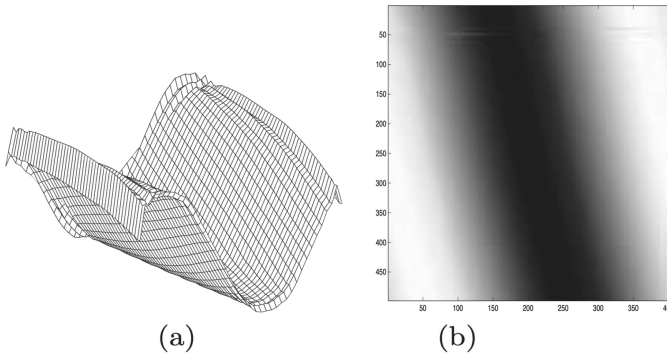


Fig. 6. Actual voltage waveform recordings, shown in 2D using (a) mesh plot and (b) gray-scale image.

1.3 Energy Demand and Load Data

Although it is us, humans, who judiciously utilize electricity according to our needs and desires, electric energy demand for a region connected to the same grid busbar naturally exhibits an oscillatory characteristic. The oscillations are in the form of hours of the day, days of the week and weeks through yearly seasons, all due to reasons such as working hours, house utilization hours or seasonal air conditioning. Of course, this particular data waveform has more random variation due to economic or population effects. Normally the load and demand tend to gradually increase together with the population. Figure 7 shows hourly electric consumption from year 2002 to 2005 in Turkey (data courtesy of Turkish Electric Power Company).

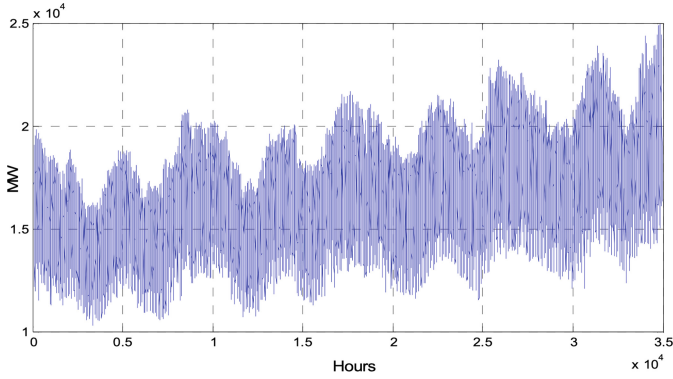
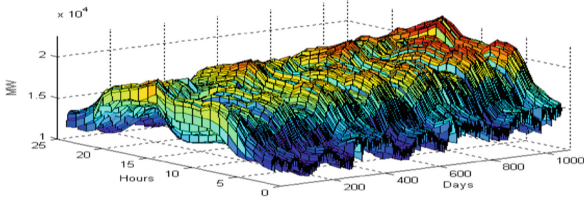
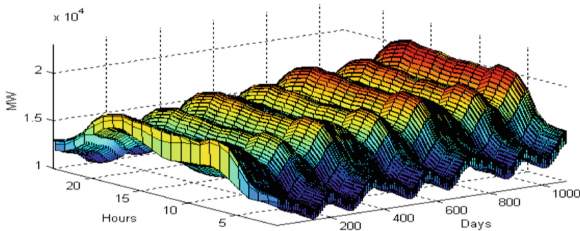


Fig. 7. Hourly electric consumption from 2002 to 2005 in Turkey.

Again, the relatively congested plot in Fig. 7 broadly indicates seasonal changes and an overall inclination to steadily grow. However, the daily and hourly variations (within a day) are not available for detailed analysis. On the other hand, when we render the data in 2D by choosing a row width corresponding to 24 h, the visualization becomes as in Fig. 8(a), which can be easily modelled as a surface in Fig. 8(b) using low order models [11].



(a)



(b)

Fig. 8. Data in Fig. 7 (a) rendered in 2D and (b) 2D modelled using low order models.

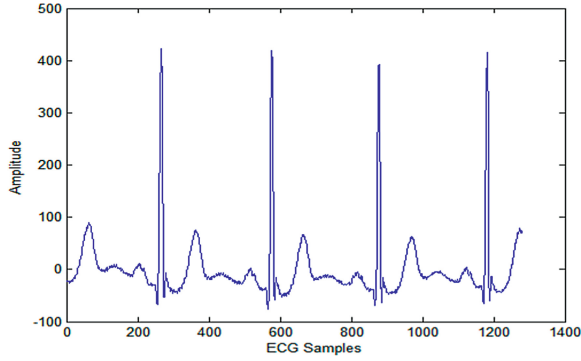


Fig. 9. A typical plot of ECG data.

1.4 ECG Data

Due to its relatively steady periodicity, a further example that enables 2D rendition is the ECG amplitude waveform (Fig. 9). The ECG data has an approximate period which can be set as the width of a 2D rendition (also known as the “waterfall plot” - see Fig. 10), as available in many off-the-shelf ECG analysis tools used by the medical doctors [12].

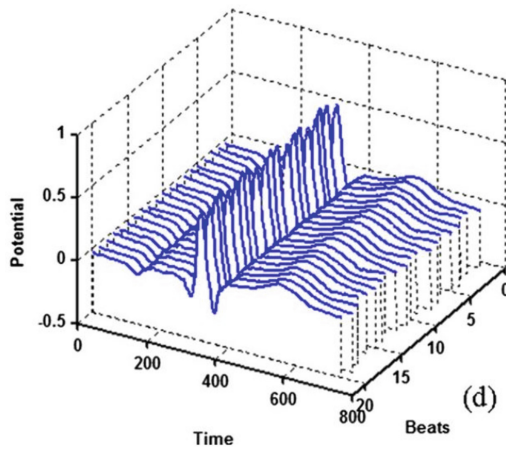


Fig. 10. A 2D rendition of the same ECG data.

2 Strength of 2D: Examples

The 2D rendition of *almost* periodic data is *cool* or visually revealing. In a majority of scholar works that are exemplified above, the 2D representations provide a clear advantage regarding analysis, detection, forecasting or compression. Here, we present a few cases of these advantages. In the later section, a mathematical reasoning of these advantages will be provided by means of autocorrelation order reductions.

2.1 Solar Radiation Models

In two different approaches, the observed solar radiation data could be better modelled in 2D as opposed to their 1D counterparts. In the first approach, simple linear or neural network models were applied for hourly forecasting. A simple 3-tap 2D predictor utilizes 1-hour-before, 1-day-before and 1-day-and-1-hour-before samples for predicting the current radiation sample in the following form:

$x_{i,j}$	$x_{i,j+1}$
$x_{i+1,j}$	$x_{i+1,j+1}$

by the simple linear predictor of:

$$x_{i+1,j+1} = a_1x_{i,j} + a_2x_{i,j+1} + a_3x_{i+1,j} \tag{5}$$

whose coefficients (a 's) can be simply obtained a 3-lag correlation information using the 3×3 matrix-vector form of:

$$\mathbf{a} = \mathbf{R}^{-1} \cdot \mathbf{r} \tag{6}$$

In an analogous way, the 3 neighboring samples can be fed to a simple 3-input neural network. It was observed that the 2D versions (as opposed to using 1D 3-past data, i.e. 3 past hours of the same day) reduces the prediction RMSE by 4.5 in the linear predictor (with an RMSE value of 41.09) and by 6 in the 3-input neural network (with an RMSE value of 39.17). What is more striking is that, if linear prediction is to be used, the efficiency of 2D 3-tap linear predictor could be achieved by a massive 62-tap 1D linear predictive filter! Or, if neural networks are compared, the prediction equality could be achieved by the 1D counterpart using 55-input neurons with 55 hidden layer neurons! This clearly shows that the 2D rendition efficiently yields daily relations as well as hourly relations.

Analogously, the 2D rendered information is modelled accurately with a sinusoidal model of only 6 variables using the following curve fit:

$$a(\text{day}) = \sin(2\pi \times \text{day}/720) + 162.1$$

$$c(\text{day}) = \sin(2\pi \times \text{day}/712) + 2.664$$

producing:

$$\text{surface}(\text{day}, \text{hour}) = a(\text{day}) \times e^{-\left(\frac{\text{hour} - 12.5}{c(\text{day})}\right)^2} \quad (7)$$

which gives an RMSE of 57.24 (see Fig. 11). For a comparison, the sinusoidal (or a polynomial, thereof) model that uses only 1D form requires 18 parameters to reach to the same RMSE value.

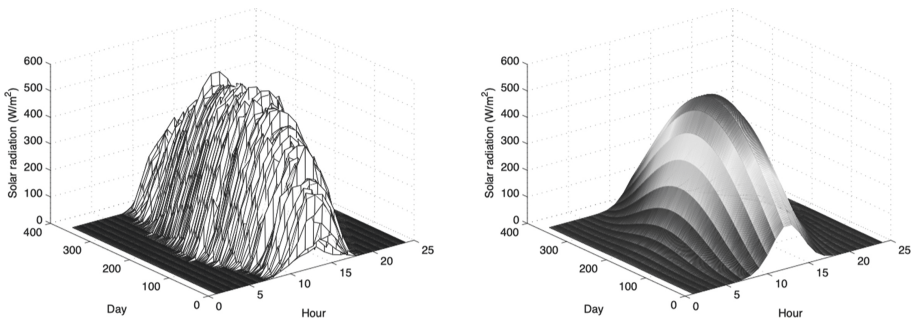


Fig. 11. Recorded solar radiation (a) in Eskisehir region and (b) its 2D model given in Eq. 7.

2.2 Power Quality Data

The strength of the 2D representation in power quality data is obviously different than that of solar radiation data, where a predictive model was necessary. Here, the engineering problem is either the *detection* (and classification) of the power quality event, or the low bandwidth compression of the recording with minimum MSE. The research in [8] provides a methodology to first render the voltage recordings in 2D (see Fig. 6) and then apply a 2D discrete wavelet transform to observe the data in four 2D subspaces: φ_{ll} , ψ_{lh} , ψ_{hl} , ψ_{hh} . These four subspaces are, indeed, horizontal and vertical applications of a low-pass and a high-pass filter. Consider one level application of a discrete wavelet transform and its output subspace images in Fig. 12 and 13.

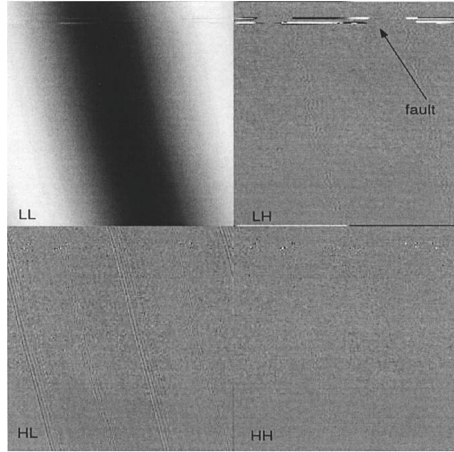


Fig. 12. One-level 2D-DWT decomposition of voltage waveform with arcing fault.

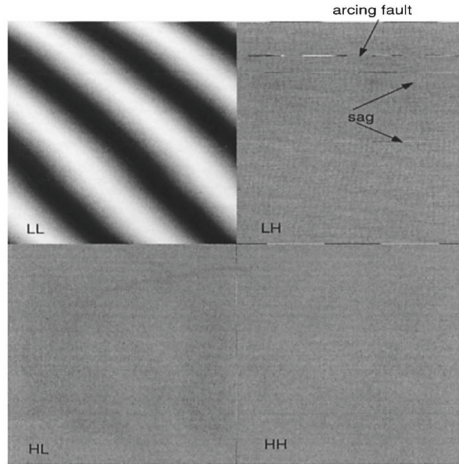


Fig. 13. One-level 2D-DWT decomposition of voltage waveform with two PQ events.

The case in Fig. 12 contains an arcing fault, which becomes clearly identifiable at the LH subband (thanks to the vertical high-pass filtering applied in that subband). The data in Fig. 13 is slightly different, as the 2D rendition was obtained using not one, but two cycles for the width of the matrix form. In that example, there is both an arcing fault and a sag event. Although the arcing faults are usually obvious regardless of the rendition, the sag here is approximately 0.5% in magnitude, and the 1D methods mostly suffer in their detection. Because of the vertical high pass filtering in the LH subband, even the slightest sag could be interpreted as an “edge” of the image, therefore it gets amplified and revealed in the corresponding subband. Consequently, making an “image” out of

the PQ data provides an extra vertical dimension to work on and provide an improved efficiency.

Another efficiency of the 2D representation of sampled voltage data arises when the slight tilt in the LL subbands of Fig. 12 and 13 are considered. These tilts appear because the actual period of the voltage waveform is *slightly* greater than the expected $1/50$ s. With a sampling frequency of 20 kHz, one period must exactly match to 400 samples (the width of the image). However, in both Fig. 12 and 13, the period was about 400.3 samples, meaning that the actual frequency of the line voltage was not 50 Hz, but it was 49.9625 Hz. Using a 1D Fourier technique, it requires 10.000 point FFT to reach to this precision. In the 2D image, a tilt of only 1° can be measured using the Hough transform [13]. This means that the frequency difference down to 49.9986 or 50.0014 Hz could be measured, which necessitates a 1D FFT of over 100.000 points. The above practical impossibilities of 1D spectral methods render the 2D approach a resourceful methodology in such subtle power quality events.

The final efficiency example of the 2D representation can be given regarding data compression for low bandwidth transmission or storage. Since many image compression methods are deliberately devised for high quality and low bandwidth compression, the 2D representation of the power quality recordings provides a compression efficiency with over 10 dB better MSE (see Fig. 14) for lossy and 9-to-5 compression ratio efficiency using lossless encoders.

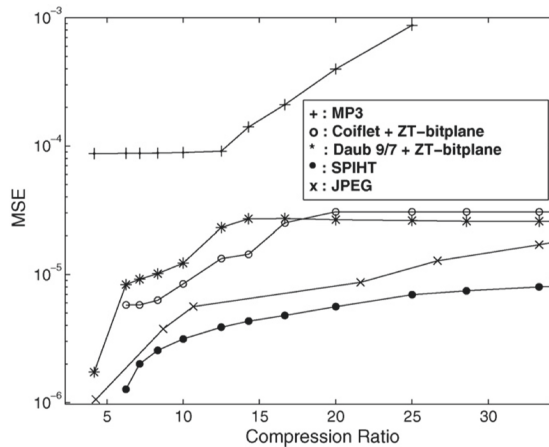


Fig. 14. MSE versus CR plots for 1D (i.e. mp3) and 2D (i.e. image) encoders.

2.3 Energy Load Data

In certain cases, such as the energy demand or load, the cyclo-stationary behavior of the data enables an efficient 2D rendition (see Fig. 7). However, the best modeling approach for these signals is not necessarily the complete 2D analytical model. In fact, splitting the data into increasing and stationary portions provides an even better efficiency. In

[11], the data of Fig. 7 is first modelled according to its increase tendency (see Fig. 15) using a weekly quadratic formula:

$$f^m(w) = 5.118w^2 + 1931w + 2454000 \tag{8}$$

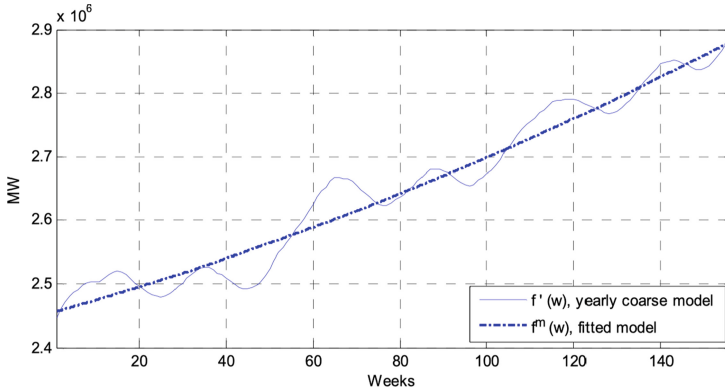


Fig. 15. Weekly averaged curve of Fig. 7 and its quadratic model.

Once the data is normalized with this inclination function, the remaining coarse fluctuations provide another 1D oscillation due to seasonal changes, which can be accurately modelled with four complex Fourier series coefficients and provide the fit as shown in Fig. 16.

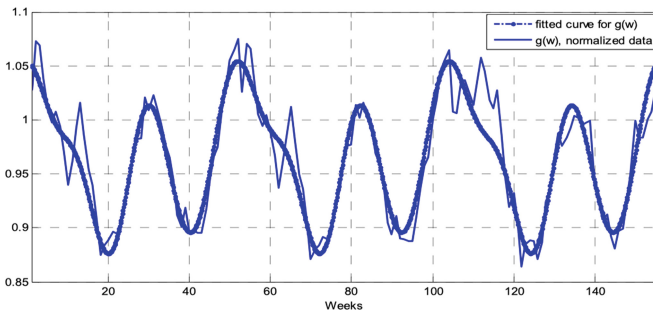


Fig. 16. Model approximation of weekly residual load variations using the Fourier series model.

After the second normalization, the remaining hourly load data can be easily modelled within a week as the 2D rendition model given in Fig. 17.

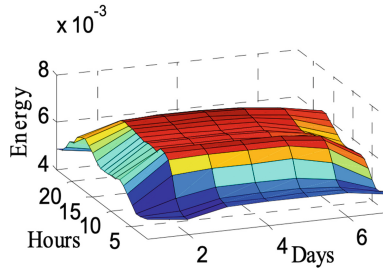


Fig. 17. Normalized hourly variations visualized in 2D within a week.

3 Conclusions and Discussions

The review of the cases described herein provides several examples where 2D rendition of the sensor outputs provide unexpected efficiency improvements even though the original data waveform could be essentially 1D. The examples of solar radiation, line voltage and energy load had been performed by the research group of the authors in different dates, whereas the ECG 2D rendition is another example which gets commonly used by the medical doctors, recently. Although the applications and the engineering problem are different in each case, the shared idea is the conversion of 1D signals into 2D matrix form according to a cyclic pattern that exists inside the data waveform. This natural (yet novel) rendition provides an efficiency, regardless of the mathematical approach or the sought-after result. For example, in solar radiation modeling, as the name indicates, the engineering problem is to find an accurate model and use it for forecasting. The linear models as in Eq. 5 and 6 or the neural network complexities in the 2D case automatically gets reduced as opposed to the overly complex counterparts in 1D. As an illustration, a 1-day before information automatically necessitates the model order to increase 24-tap (corresponding to 24 h) more. Another day information, another 24 more taps for the prediction order. However, for the 2D model, they are nothing more than 1 more addition to the tap order.

As explained herein, the sampled voltage waveforms for power quality analysis are a different animal, where modeling or prediction is not an issue, but detection and classification are the main problems. In that case, the 2D rendition opens completely different doors by revealing the vertical degree of freedom, which easily provides image processing tools for detecting faults such as voltage sag/swell or slight error in the AC period/frequency. In some of such cases, the 1D methods not only require orders of magnitude more complexity in spectral methods, but they sometimes completely lack the possibility of making any reasonable detection, whatsoever.

The last example that was conducted within the authors' research group was the energy load/demand modeling. There, the cyclo-stationary behavior was gradually oscillating with seasons, and also gradually increasing in overall by years. Therefore, a normalization according to these gradual changes were first applied, then the residual periodic structure within one week was modeled as in Fig. 17. Again, the total model orders were orders of magnitude smaller than directly modelling Fig. 7 using a 1D method. In

fact, it was found out that the data in Fig. 7 could not be used for long-term (but hourly precision) forecasting with any linear 1D model with a model size below 1000 taps.

We conclude that it is beneficial to render the sensor output data to 2D whenever possible (with a cyclo-stationary behavior). Candidates for such include the induction motor health monitoring, society consumption of agricultural commodities, financial data, genomic data, etc. We further claim that even data that contains no pronounced cyclic behavior can be rendered in 2D (as long as there exists a decisive and natural period), such as the wind speed readings of a wind turbine, where a segment of 24 h is the natural repetition period. Application of this approach to biomedical case of ECG also improves the argument. Further research of such applications remains an open problem.

Acknowledgement. This work was supported by Eskisehir Technical University, Scientific Research Project Funds under contract no: 20ADP181.

References

1. Widen, J., Munkhammar, J.: Solar Radiation Theory. Uppsala University (2019)
2. Kalogirou, S.A.: Environmental Characteristics (Chapter) in Solar Energy Engineering, 2nd edn. Academic Press, Cambridge (2014)
3. Photovoltaic Geographical Information System – web resource (2019, updated). https://re.jrc.ec.europa.eu/pvg_tools/en/tools.html
4. Hocaoglu, F.O., Gerek, O.N., Kurban, M.: Hourly solar radiation forecasting using optimal coefficient 2D linear filters and feed-forward neural networks. *Sol. Energy* **82**(8), 714–726 (2008)
5. Hocaoglu, F.O., Gerek, O.N., Kurban, M.: A 2 dimensional solar radiation model. In: IEEE 16th Signal Processing, Communication and Applications Conference (2008)
6. Hocaoglu, F.O., Fidan, M., Gerek, O.N.: A novel Fourier based solar radiation model. *ICIC Express Lett.* **3**, 1101–1106 (2009)
7. Fidan, M., Hocaoglu, F.O., Gerek, O.N.: Harmonic analysis based hourly solar radiation forecasting model. *IET Renew. Power Gener.* **9**(3), 218–227 (2014)
8. Ece, D.G., Gerek, O.N.: Power quality event detection using joint 2D wavelet subspaces. *IEEE Trans. Instrum. Meas.* **53**(4), 1040–1046 (2004)
9. Gerek, O.N., Ece, D.G.: 2D analysis and compression of power quality event data. *IEEE Trans. Power Deliv.* **19**(2), 791–798 (2004)
10. Gerek, O.N., Ece, D.G.: Compression of power quality event data using 2D representation. *Electr. Power Syst. Res.* **78**(6), 1047–1052 (2008)
11. Filik, Ü.B., Gerek, O.N., Kurban, M.: Hourly forecasting of long-term electric energy demand using a novel modeling approach. *ICIC Express Lett.* **4**(4), 115–118 (2010)
12. Azaace, F., Clifford, G., McSharry, P.: *Advanced Methods and Tools for ECG Data Analysis*. Artech, Boston (2006)
13. Shehata, A., et al.: A survey on Hough transform, theory, techniques and applications. *IJCSI* **12**(1) (2015). [arXiv:1502.02160](https://arxiv.org/abs/1502.02160)